Annals of Biomedical Engineering (© 2023)
https://doi.org/10.1007/s10439-023-03167-4

BMES BIOMEDICAL ENGINEERING SOCIETY

Original Article

Abnormal Wall Shear Stress Area is Correlated to Coronary Artery Bypass Graft Remodeling 1 Year After Surgery

NHIEN TRAN-NGUYEN,[1] ANDREW T. YAN,[2,3] STEPHEN FREMES,[4,5,6] PIERO TRIVERIO,[1,7,8] and LAURA JIMENEZ-JUAN[2,3,6]

[1]Institute of Biomedical Engineering, University of Toronto, Toronto, ON, Canada; [2]Department of Medical Imaging, University of Toronto, Toronto, ON, Canada; [3]St. Michael's Hospital, Toronto, ON, Canada; [4]Department of Surgery, University of Toronto, Toronto, ON, Canada; [5]Sunnybrook Health Sciences Centre, Toronto, ON, Canada; [6]Sunnybrook Research Institute, Toronto, ON, Canada; [7]Department of Electrical and Computer Engineering, University of Toronto, Toronto, ON, Canada; and [8]Department of Mechanical and Industrial Engineering, University of Toronto, Toronto, ON, Canada

(*Received 17 November 2022; accepted 12 February 2023*)

Associate Editor Arash Kheradvar oversaw the review of this article.

Abstract—Coronary artery bypass graft surgery is a common intervention for coronary artery disease; however, it suffers from graft failure, and the underlying mechanisms are not fully understood. To better understand the relation between graft hemodynamics and surgical outcomes, we performed computational fluid dynamics simulations with deformable vessel walls in 10 study participants (24 bypass grafts) based on CT and 4D flow MRI one month after surgery to quantify lumen diameter, wall shear stress (WSS), and related hemodynamic measures. A second CT acquisition was performed one year after surgery to quantify lumen remodeling. Compared to venous grafts, left internal mammary artery grafts experienced lower abnormal WSS (< 1 Pa) area one month after surgery (13.8 vs. 70.1%, $p = 0.001$) and less inward lumen remodeling one year after surgery (− 2.4% vs. − 16.1%, $p = 0.027$). Abnormal WSS area one month post surgery correlated with percent change in graft lumen diameter one year post surgery ($p = 0.030$). This study shows for the first time prospectively a correlation between abnormal WSS area one month post surgery and graft lumen remodeling 1 year post surgery, suggesting that shear-related mechanisms may play a role in post-operative graft remodeling and might help explain differences in failure rates between arterial and venous grafts.

Keywords—Computational fluid dynamics, Hemodynamics, Graft failure.

Address correspondence to Nhien Tran-Nguyen, Institute of Biomedical Engineering, University of Toronto, Toronto, ON, Canada. Electronic mail: nhien.tran.nguyen@mail.utoronto.ca

ABBREVIATIONS

CABG	Coronary artery bypass graft
CFD	Computational fluid dynamics
CT	Computed tomography
LIMA	Left internal mammary artery
MRI	Magnetic resonance imaging
RA	Radial artery
SVG	Saphenous vein graft
WSS	Wall shear stress

INTRODUCTION

Coronary artery bypass graft (CABG) surgery is an established intervention for patients with coronary artery disease.[20] The operation entails the grafting of one or more harvested blood vessels to bypass native coronary artery stenoses and to improve myocardial perfusion. Despite the benefits of the surgery, it continues to be limited by the occurrence of graft failure, or by the total occlusion of the implanted bypass graft. Approximately 25% of vein grafts fail within the first 2 years of surgery, putting patients at increased risk of adverse cardiac events such as myocardial infarction or even death.[18] Unfortunately, the underlying mechanisms behind graft failure are not yet fully understood.[8]

Published online: 04 March 2023

It is thought that hemodynamics may play a role in the remodeling processes that lead to graft failure.[32] The endothelium plays a major role in vascular homeostasis and has extensively been shown to be sensitive to wall shear stress (WSS) and other hemodynamic quantities.[2,10] However, standard non-invasive clinical methods are unable to measure relevant hemodynamic quantities in the coronary arteries and bypass grafts. For example, phase contrast MRI and 4D flow MRI can be used to measure blood flow velocities *in vivo*. However, these imaging modalities are unable to resolve flows in smaller caliber vessels such as the coronary arteries due to their spatial resolution.[19] While coronary CT angiography does have the spatial resolution necessary to image these vessels, it can only provide anatomic information about the vessel lumen rather than functional information about blood flow.[27]

One emerging approach to non-invasively quantify hemodynamics in small vessels is computational fluid dynamics (CFD). By combining blood flow rates measured using MRI, blood vessel anatomy obtained from CT, and the Navier–Stokes equations that govern the motion of fluids, CFD simulations provide a powerful, non-invasive tool to estimate quantitative measures of relevant hemodynamic quantities that are difficult to obtain using medical imaging alone.[1]

Computational fluid dynamics simulations have previously been applied to other cardiovascular pathologies and, more recently, to CABG surgery to better understand potential pathological mechanisms; however, many studies are limited by their retrospective nature. One previous CFD study by Ramachandra *et al.* in 5 CABG patients ranging from 1 to 17 years post surgery found differences in average WSS and abnormal WSS area between arterial and venous grafts.[23] However, no comparison was made between graft hemodynamics and subsequent remodeling or failure, and the wide variance in the timing of post-operative imaging could have resulted in significant differences in the degree of remodeling and disease progression among the grafts. Another retrospective CFD study was performed by Khan *et al.* in 15 CABG patients with both healthy and stenosed saphenous vein grafts (SVG).[16] While the authors demonstrated that normalized WSS was lower in digitally reconstructed pre-diseased SVG segments compared to patent SVGs, one limitation of their study was the lack of imaging prior to failure. To our knowledge, no previous CFD study performed in the context of CABG surgery has shown prospectively a correlation between hemodynamic quantities and subsequent graft remodeling or failure.

We have previously reported differences in CFD-derived WSS and flow rate 1 month after CABG surgery across different graft types and implantation territories in 10 study participants.[29] In the present study, we investigate the relationships between CFD-derived hemodynamic quantities obtained one month post surgery and the degree of graft lumen remodeling 1 year post surgery in these study participants, which, to our knowledge, is the largest prospective CFD study of its kind in the context of CABG surgery. As graft remodeling can be a precursor to failure, investigating its relation to perioperative hemodynamics could help reveal potential mechanisms behind graft failure—the first step in improving surgical outcomes. We hypothesize that greater exposure of grafts to abnormally low WSS one month post surgery is correlated with the degree of graft lumen remodeling 1 year post surgery.

MATERIALS AND METHODS

Study Population

This study was approved by the research ethics board of the Sunnybrook Health Sciences Centre and by the institutional review board at the University of Toronto. All procedures followed were in accordance with the Helsinki Declaration of 1975. Figure 1 shows a flow diagram of the study. In this single-center prospective study, 13 consecutive eligible participants presenting to the Sunnybrook Health Sciences Centre for CABG surgery from November 2017 to August 2018 were identified and enrolled into the study. Informed consent was obtained from all participants in the study. The inclusion criteria were age > 18 years, ability to provide informed consent, no prior CABG surgery, left ventricular ejection fraction $> 20\%$, and plan to have at least one venous and one arterial graft implanted. The exclusion criteria were any contraindication to cardiac CT or MRI, such as allergy to contrast media, estimated glomerular filtration rate < 30 mL/min, uncontrolled atrial fibrillation precluding proper gating of the study, pregnant or breastfeeding women, women of child-bearing age, claustrophobia, and metallic implants capable of interfering with MRI.

Imaging Acquisition

Figure 2 summarizes the methodology used, which expanded on a previous study.[29] After CABG surgery, study participants underwent cardiac CT angiography and 4D flow MRI 3–6 weeks post surgery, as well as a second CT acquisition 9–15 months after surgery. Cardiac CT studies were performed on a 320-detector row CT scanner (Aquilion One; Canon Medical Sys-

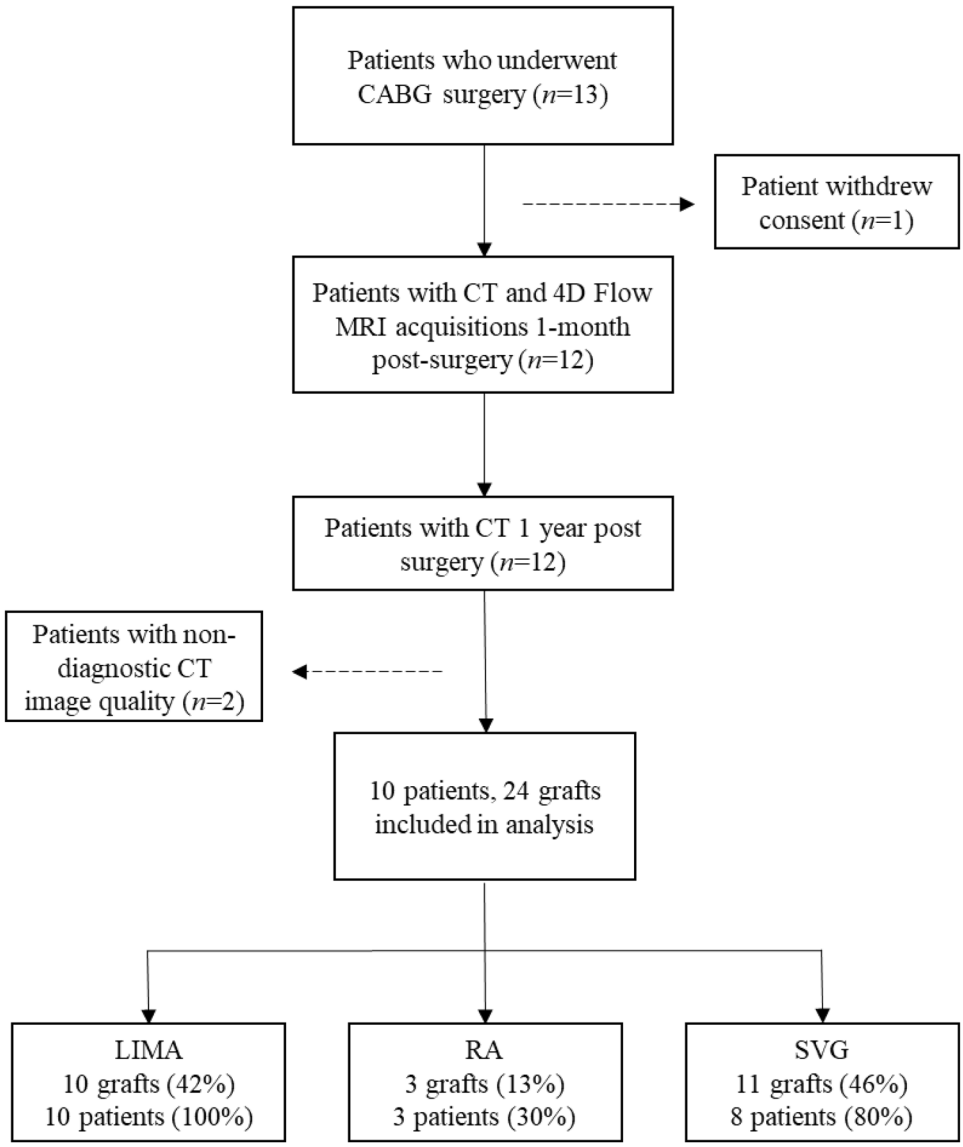

FIGURE 1. Flow diagram of the study. *CABG* coronary artery bypass graft, *CT* computed tomography, *MRI* magnetic resonance imaging, *LIMA* left internal mammary artery, *RA* radial artery, *SVG* saphenous vein graft.

tems, Markham, Ontario, Canada) with a slice thickness of 0.5 mm. Patient preparation for heart rate control, intravenous contrast protocol, and choice of scan parameters were performed following prior studies.[3,15]

After the first CT acquisition, 4D flow MRI was performed with a 3 Tesla MRI system (Magneton PRISMA, Siemens, Erlangen, Germany) within the same day using a 4D flow imaging sequence with retrogating and adaptive navigator respiratory gating. Imaging parameters were as follows: encoding velocity = 150 cm/s, field of view = 200–420 mm × 248–368 mm, spatial resolution = 1.9–3.5 × 2.0–3.2 × 1.8–3.5 mm, temporal resolution = 39.9–47.2 ms, flip angle = 8°. No gadolinium contrast agent was administered.

Three-Dimensional Model Reconstruction

The CT images obtained 1 month and 1 year post surgery were segmented using SimVascular (Stanford University, Stanford, California), an open-source software for cardiovascular modeling,[30] to generate three-dimensional models of the aorta, supra-aortic vessels, coronary arteries, and surgically implanted bypass grafts. The vessel reconstructions were verified by a cardiothoracic radiologist with 10 years of experience in cardiovascular imaging (L.J.J.) by superimposing the generated reconstructions onto the original

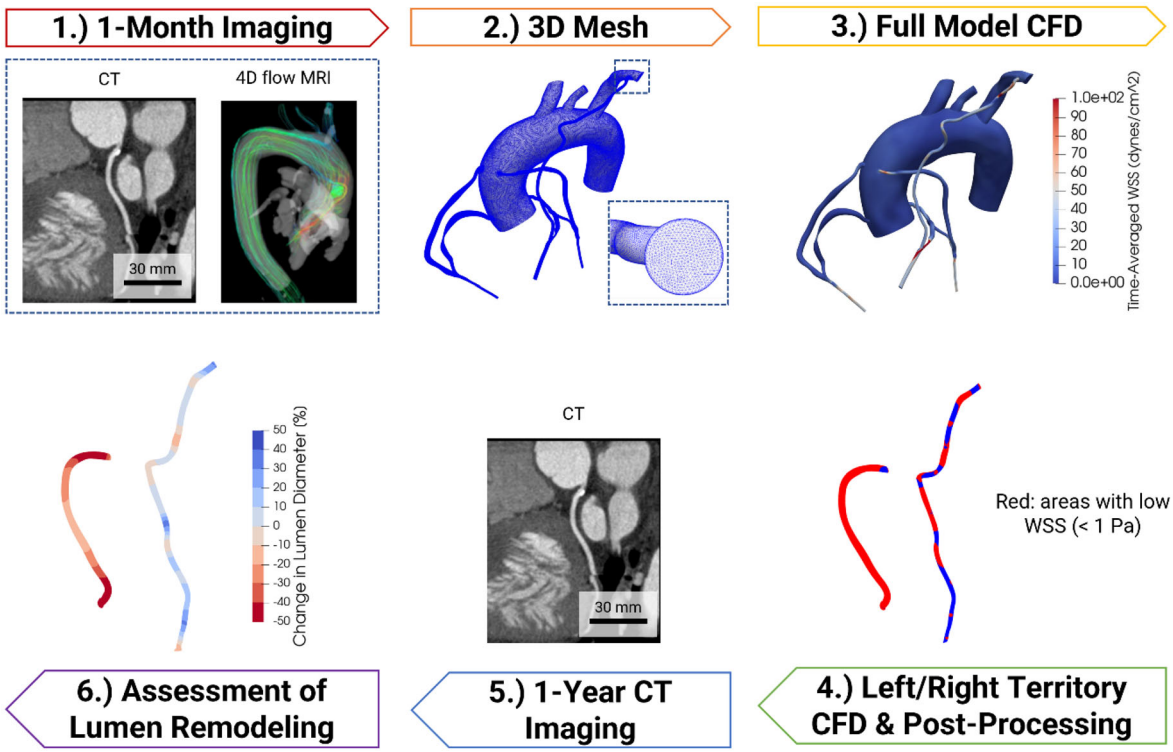

FIGURE 2. Visual depiction of the study methodology. In step 1, cardiac CT angiography and 4D flow MRI are acquired 1 month after coronary artery bypass graft surgery. A 3D reconstruction of the vessels of interest is performed and used to generate a 3D computational mesh (step 2). Based on the generated mesh, a computational fluid dynamics (CFD) simulation of the aorta, coronary arteries, and bypass grafts is performed assuming fixed vessel walls (step 3). More precise CFD simulations of the left and right coronary territories with compliant vessel walls are then performed (step 4), followed by post-processing to obtain relevant hemodynamic quantities such as abnormal wall shear stress (WSS) area. In step 5, a second coronary CT angiography is acquired 1 year after the initial surgery. A second 3D reconstruction is then performed on the 1-year images to assess the degree of lumen remodeling between the 1-month and 1-year time points (step 6).

CT images using 3D Slicer (Harvard University, Cambridge, Massachusetts). Average graft lumen diameters at 1 month and 1 year post surgery were measured based on these geometric reconstructions using VMTK (Orobix, Bergamo, Italy) and ParaView (Kitware, Clifton Park, New York).

Computational Fluid Dynamics Simulations and Post-processing

Based on the generated vessel reconstructions 1 month after surgery, three-dimensional meshes for the CFD simulations were generated using SimVascular. Local mesh element size and time step size were determined for each study participant through spatial and temporal resolution studies to determine the coarsest mesh and time step required for convergence of average flow rate in each vessel within 5%. The aorta and supra-aortic branches had a target element size of 1.00 mm, and the coronary arteries and bypass grafts had target element sizes ranging from 0.16 to 0.25 mm. Time step size was set ranging from 0.1 to 0.5 ms. Results from representative mesh and temporal independence studies are shown in the Supplemental Materials (Figs. S1–S2, Tables S1–S2).

Segment (Medviso, Lund, Sweden)[13] and FourFlow (Lund University, Lund, Sweden)[12] were used to extract blood flow rate from the 4D flow MRI data. The pulsatile blood flow rate in the ascending aorta was then imposed as an inlet boundary condition to the simulation with a parabolic flow profile. A 3-element Windkessel model was used to estimate outlet boundary conditions in the descending aorta and in supra-aortic branches, which has been shown to be sufficient to recreate realistic flow and pressure waveforms in the aorta.[22] A lumped parameter model developed and validated in a separate study was used to set outlet boundary conditions in the coronary arteries and bypass grafts, which incorporates the effects of intramyocardial pressure on coronary flow and is used in other similar works that model the coronary arteries.[17,28] Model values were chosen and iteratively tuned to match patient-measured blood pressure after MRI acquisition, which were also validated against 4D flow MRI measurements in a previous study.[29] An initial

estimate for the systemic vascular resistance seen from the ascending aorta was computed by dividing each participant's mean arterial pressure by their cardiac output, where cardiac output was determined by multiplying 4D flow MRI-measured stroke volume by the participant's heart rate measured after the MRI scan. The total coronary resistance set to 24 times the systemic vascular resistance under the assumption that 4% of the cardiac output went to the coronary arteries.[24] This 4% assumption is applied to all patients due to the challenges of estimating coronary flows from 4D flow MRI and is commonly used in similar works that model the coronary arteries.[16,23] The total systemic vascular capacitance was initially set to be 0.001 cm^5/dyne, while the coronary capacitances were initially set to be 3.6×10^{-5} cm^5/dyne and 2.5×10^{-5} cm^5/dyne for the left and right coronary territories, respectively.[24] Total resistance and capacitance were then split among vessel outlets according to Murray's law based on their relative cross-sectional area, and these values were manually tuned for each participant to match cuff-measured blood pressure after MRI imaging.[31]

Two types of simulations were performed using SimVascular for each study participant. An initial CFD simulation was performed on the full model of the aorta, supra-aortic branches, coronary arteries, and bypass grafts assuming rigid vessel walls. Subsequent simulations were performed on the individual left and right coronary territories using the coupled momentum method for compliant vessel walls.[6] For the inlet flow boundary conditions, flow rates at the origin of the left and right coronary trees were obtained from the full model CFD, assuming a Womersley flow profile. The elastic modulus for each vessel was set according to literature values as follows: 1.15 MPa for coronary arteries, 1.4 MPa for left internal mammary arteries (LIMA), 5 MPa for saphenous veins (SVG), and 2.68 MPa for radial arteries (RA).[23,25] Performing separate rigid wall and compliant wall simulations was necessary, since a compliant wall simulation on the full model would have significantly higher computational cost.[4] Our previous study with the same patient cohort validated blood flow rate in cross-sections of the aorta obtained from compliant wall simulations against 4D flow MRI.[29] The average relative error for all planes ranged from 3.12 to 6.58%, indicating good agreement between simulation results and 4D flow MRI.

From the results of the compliant wall CFD simulations, the flow rate and WSS on the walls of each graft were computed with SimVascular. Average WSS was calculated by averaging WSS temporally over one cardiac cycle and spatially across the graft walls using ParaView and MATLAB (MathWorks, Natick, Massachusetts). The percent area of the graft walls exposed to WSS below 0.5 or 1 Pa, henceforth referred to as abnormal WSS area, was also computed. As there is no consensus on a threshold for abnormally-low WSS, two thresholds (0.5 and 1 Pa) were chosen based on estimates of atherosclerotic WSS thresholds in previous studies. In particular, the PREDICTION clinical study on 374 patients with acute coronary syndrome found that a low endothelial shear stress of < 1 Pa was associated with increased plaque burden and worsening of luminal obstructions, while *in vitro* vascular biology experiments involving flow typically apply shear stress magnitudes of < 0.5 Pa as atheroprone stimuli to study endothelial dysfunction.[9,26] We have previously presented results from the 1-month CFD simulations performed in the study cohort, which reports differences in abnormal WSS area (< 1 Pa) between different graft types and the relationship of abnormal WSS area to graft diameter and flow rate.[29] Herein, we will compare the 1-month hemodynamic measures to 1-year changes in graft lumen diameter and quantify how the choice of abnormal WSS threshold influences these comparisons.

Statistical Analysis

All analyses were performed using JASP (version 0.16.4, University of Amsterdam, Amsterdam, Netherlands). Linear mixed models were used for significance testing and correlation analyses, with patient used as a random effects variable to account for the clustering of data.[5] Significance testing was performed to look for differences in hemodynamic and anatomic measures between graft tissue types (arterial vs. venous) and different source vessels (LIMA vs. SVG, LIMA vs. non-LIMA). Correlation analyses were performed to examine the relationship between hemodynamic measures and relative change in graft lumen diameter. A p-value of < 0.05 was considered significant.

RESULTS

Patient Characteristics

Thirteen participants were enrolled in the study and three were excluded: one due to withdrawn consent prior to the 1-month follow-up and two due to non-diagnostic CT image quality. The final cohort consisted of 10 participants with 24 grafts: 10 left internal mammary arteries (LIMA), 11 saphenous vein grafts (SVG), and 3 radial arteries (RA). All patients had a LIMA graft used to bypass the left anterior descending artery, as per routine clinical guidelines, while SVG

and RA grafts were used to bypass other coronary arteries in both the left and right coronary territories. Surgical decision-making for each patient resulted in more SVGs than RA grafts in the study cohort due to the ability of SVGs to reach any target vessel on the heart and their relative insensitivity to competitive flow in native coronary arteries compared to RA grafts.[8] A flow diagram of the study is shown in Fig. 1. Baseline patient characteristics are summarized in Table 1.

Hemodynamics 1 Month Post Surgery

Table 2 summarizes the hemodynamic quantities obtained from the 1-month CFD simulations, including graft flow rate, average WSS, and abnormal WSS area (< 0.5 Pa and < 1 Pa). Table 3 displays results of significance testing between different graft types for all measures. Arterial grafts tended to experience higher average WSS ($p = 0.004$) and lower abnormal WSS area ($p = 0.004$ for 0.5 Pa threshold; $p = 0.001$ for 1 Pa threshold) compared to venous grafts, and these differences are primarily driven by the LIMA grafts having higher average WSS than SVGs ($p = 0.002$).

Distributions of graft wall area exposed to abnormal WSS (< 0.5 Pa and < 1 Pa) vary among different graft types and implantation territories, which are illustrated in Fig. 3. SVGs implanted to the left territory are more exposed to abnormal WSS area ($48.8 \pm 33.1\%$ for 0.5 Pa threshold; $77.8 \pm 35.3\%$ for 1 Pa threshold) compared to the LIMA grafts ($0.9 \pm 1.8\%$ for 0.5 Pa threshold; $13.8 \pm 26.6\%$ for 1 Pa threshold). On the other hand, RA grafts to the right territory are not exposed to much abnormal WSS ($1.6 \pm 2.2\%$ for 0.5 Pa threshold; $6.0 \pm 8.4\%$ for 1 Pa threshold), while SVGs to the right territory have mixed exposure ($24.9 \pm 41.7\%$ for 0.5 Pa threshold; $49.5 \pm 43.2\%$ for 1 Pa threshold). For grafts that

TABLE 1. Patient demographics.

Parameter	No. of patients ($n = 10$)
Age (years)*	64.6 ± 8.5
Male sex	9 (90%)
Height (cm)*	174 ± 7
Weight (kg)*	86 ± 18
Body mass index (kg/m^2)*	28 ± 6
Cardiovascular risk factors	
Systolic blood pressure (mmHg)*	135 ± 17
Diastolic blood pressure (mmHg)*	82 ± 13
Diabetes	6 (60%)
Hypertension	8 (80%)
Dyslipidemia	9 (90%)
History of smoking	6 (60%)
Pre-operative medications	
ACE inhibitor	5 (50%)
Angiotensin receptor blocker	1 (10%)
Beta-blocker	9 (90%)
Calcium channel blocker	1 (10%)
Statin	9 (90%)
ASA	10 (100%)
Thienopyridine	2 (20%)
Vitamin K antagonist	0 (0%)
Direct oral anticoagulant	0 (0%)
Concomitant at follow-up imaging	
ACE inhibitor	3 (30%)
Angiotensin receptor blocker	1 (10%)
Beta-blocker	8 (80%)
Calcium channel blocker	2 (20%)
Statin	10 (100%)
ASA	10 (100%)
Thienopyridine	5 (50%)
Vitamin K antagonist	0 (0%)
Direct oral anticoagulant	0 (0%)
Days between surgery and 1-month follow-up imaging*	40 ± 7.9
Days between surgery and 1-year follow-up imaging*	377 ± 16.7

Unless indicated with an asterisk, data are presented as the number of patients, with percentages in parentheses. Data with an asterisk are presented as mean ± standard deviation.

TABLE 2. Summary of hemodynamic and anatomic measures for the entire cohort of grafts (n = 24) and among different graft source vessels.

Measure	All (n = 24)	LIMA (n = 10)	RA (n = 3)	SVG (n = 11)
Graft flow rate [mL/min]	48.9 ± 24.3	54.1 ± 24.8	69.4 ± 24.1	38.6 ± 20.4
Average WSS [Pa]	2.76 ± 2.52	4.35 ± 2.36	3.75 ± 3.54	1.05 ± 1.00
Abnormal WSS Area (< 0.5 Pa) [%]	20.0 ± 31.3%	0.9 ± 1.8%	1.7 ± 1.5%	42.3 ± 35.2%
Abnormal WSS Area (< 1 Pa) [%]	41.8 ± 42.5%	13.8 ± 26.6%	31.8 ± 45.0%	70.1 ± 37.7%
1-month graft lumen diameter [mm]	2.85 ± 0.68	2.33 ± 0.32	2.87 ± 0.53	3.33 ± 0.62
1-year graft lumen diameter [mm]	2.50 ± 0.65	2.29 ± 0.48	2.09 ± 0.27	2.81 ± 0.74
1-year change in average lumen diameter [%]	− 11.4 ± 15.5%	− 2.4 ± 11.3%	− 24.6 ± 22.5%	− 16.1 ± 13.4%

All hemodynamic measures were obtained from the 1-month CFD simulations.[29] Data presented as mean ± standard deviation.

TABLE 3. Summary of significance testing of graft anatomic and hemodynamic measures.

Measure and comparison	Group 1	Group 2	p-value
Graft flow rate [mL/min]			
Arterial vs. venous	57.6 ± 24.6	38.6 ± 20.4	p = 0.053
LIMA vs. non-LIMA	54.1 ± 24.8	45.2 ± 24.1	p = 0.393
LIMA vs. SVG	54.1 ± 24.8	38.6 ± 20.4	p = 0.125
Average WSS [Pa]			
Arterial vs. venous	4.2 ± 2.5	1.0 ± 1.0	**p = 0.004****
LIMA vs. non-LIMA	4.3 ± 2.4	1.6 ± 2.0	**p = 0.048***
LIMA vs. SVG	4.3 ± 2.4	1.0 ± 1.0	**p = 0.002****
Abnormal WSS Area (< 0.5 Pa) [%]			
Arterial vs. venous	1.1 ± 1.7%	42.3 ± 35.2%	**p = 0.004****
LIMA vs. non-LIMA	0.9 ± 1.8%	33.6 ± 35.4%	**p = 0.008****
LIMA vs. SVG	0.9 ± 1.8%	42.3 ± 35.2%	**p = 0.004****
Abnormal WSS Area (< 1 Pa) [%]			
Arterial vs. venous	17.9 ± 30.5%	70.1 ± 37.7%	**p = 0.001****
LIMA vs. non-LIMA	13.8 ± 26.6%	61.9 ± 40.9%	**p = 0.004****
LIMA vs. SVG	13.8 ± 26.6%	70.1 ± 37.7%	**p = 0.001****
1-month graft lumen diameter [mm]			
Arterial vs. venous	2.45 ± 0.42	3.33 ± 0.62	**p = 0.003****
LIMA vs. non-LIMA	2.33 ± 0.32	3.23 ± 0.62	**p = 0.003****
LIMA vs. SVG	2.33 ± 0.32	3.33 ± 0.62	**p = 0.002****
1-year graft lumen diameter [mm]			
Arterial vs. venous	2.24 ± 0.44	2.81 ± 0.74	p = 0.080
LIMA vs. non-LIMA	2.29 ± 0.48	2.65 ± 0.72	p = 0.240
LIMA vs. SVG	2.29 ± 0.48	2.81 ± 0.74	p = 0.149
1-year change in average lumen diameter [%]			
Arterial vs. venous	− 7.5 ± 16.6%	− 16.1 ± 13.4%	p = 0.181
LIMA vs. non-LIMA	− 2.4 ± 11.3%	− 17.9 ± 15.1%	**p = 0.028***
LIMA vs. SVG	− 2.4 ± 11.3%	− 16.1 ± 13.4%	**p = 0.027***

Grouped measures are presented as mean ± standard deviation.
Significant p-values are boldfaced, with the number of asterisks indicating the significance level (*p < 0.05, **p < 0.01, ***p < 0.001).

contained regions exposed to abnormal WSS, these areas tended to occur diffusely rather than localizing at a particular region. The choice of threshold for abnormal WSS does not appear to affect the abnormal WSS area computed in most grafts with the exception of 1–2 grafts per source vessel (LIMA, SVG, and RA).

Degree of Graft Lumen Remodeling 1 Year Post Surgery

Figure 4 shows a graphical representation of the percent 1-year lumen diameter change of all grafts in the study. As a whole, the cohort of grafts experienced inward lumen remodeling (− 11.4 ± 15.5%). There were differences in the degree of remodeling experienced by different graft types, with greater inward remodeling observed in SVGs and RAs (− 16.1 ± 13.4% and − 24.6 ± 22.5%, respectively). On the other hand, most LIMA grafts tended to experience little remodeling (− 2.4 ± 11.3%). Some degree of outward remodeling was observed in 5 out of 10 LIMA grafts (50%).

Table 2 reports the mean 1-month and 1-year graft lumen diameters and the relative change, and Table 3 reports p-values for significance testing between different graft types. Arterial grafts tended to have

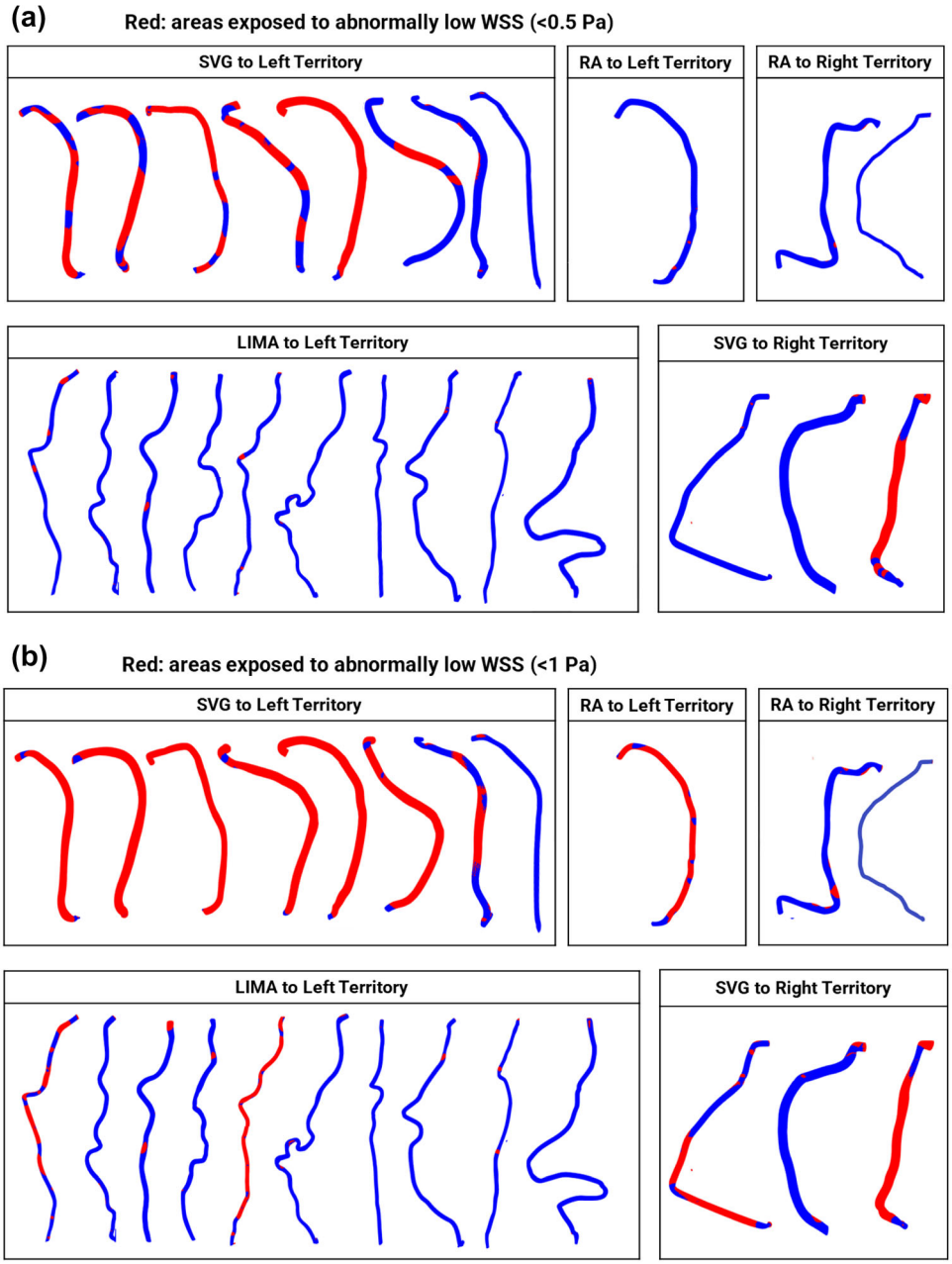

FIGURE 3. Graphical illustration of the vessel wall area exposed to abnormal WSS (< 0.5 Pa in (a), < 1 Pa in (b)) highlighted in red for all 24 grafts included in this study.[29] Grafts are grouped by type of source vessel and implantation territory. Grafts are not to scale due to variation in graft length. *LIMA* left internal mammary artery, *RA* radial artery, *SVG* saphenous vein graft.

smaller 1-month lumen diameters compared to venous grafts (2.45 ± 0.42 mm vs. 3.33 ± 0.62 mm, $p = 0.003$), and LIMA grafts had smaller 1-month lumen diameter (2.33 ± 0.32 mm) compared to non-LIMA grafts (3.23 ± 0.62 mm, $p = 0.003$) and SVGs (3.33 ± 0.62 mm, $p = 0.002$). While there were no differences in the 1-year graft lumen diameters among arterial vs. venous grafts (2.24 ± 0.44 mm vs. 2.81 ± 0.74 mm, $p = 0.080$), LIMA vs. non-LIMA grafts (2.29 ± 0.48 mm vs. 2.65 ± 0.72 mm, $p = 0.240$), and LIMA vs. SVG (2.29 ± 0.48 mm vs. 2.81 ± 0.74 mm, $p = 0.149$), there were differences in the percent lumen diameter change that they experienced. LIMA grafts experienced less inward remodeling (− 2.4 ± 11.3%) compared to non-LIMA grafts (− 17.9 ± 15.1%, $p = 0.028$) and SVGs (− 16.1 ± 13.4%, $p = 0.027$). No significant differences were found in the change in average lumen diameter for arterial vs. venous grafts (− 7.5 ± 16.6% vs. − 16.1 ± 13.4%, $p = 0.181$). Since there appear to

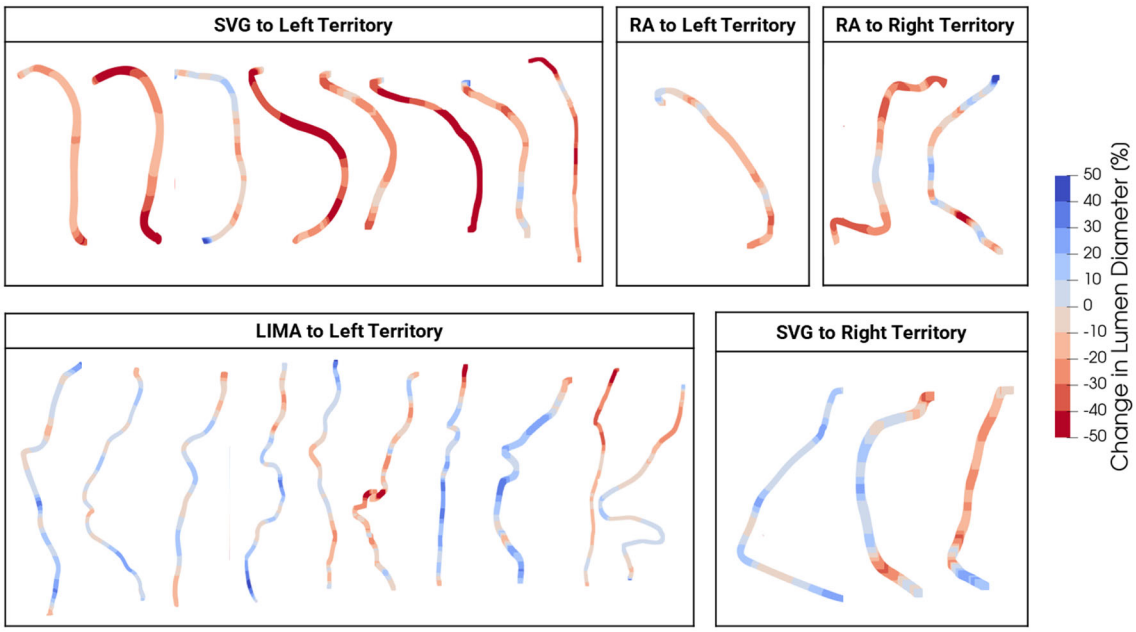

FIGURE 4. Graphical illustration of the relative change in lumen diameter between 1-month and 1-year post-operative timepoints for all 24 grafts included in the study. Grafts are grouped by type of source vessel and implantation territory. Grafts are not to scale due to variation in graft length. *LIMA* left internal mammary artery, *RA* radial artery, *SVG* saphenous vein graft.

TABLE 4. Results from linear regression analysis between 1-month measures and 1-year relative change in graft lumen diameter.

Measure	*p*-value	Univariate parameter estimate	Standard error
Graft flow rate [mL/min]	$p = 0.106$	0.298	0.133
Average WSS [Pa]	$p = 0.073$	2.694	1.278
Abnormal WSS Area (< 0.5 Pa) [%]	$p = 0.095$	− 0.173	0.099
Abnormal WSS Area (< 1 Pa) [%]	**$p = 0.030$***	− 0.187	0.069

Significant p-values are boldfaced, with the number of asterisks indicating the significance level (*$p < 0.05$).

be differences in both shear exposure 1 month after surgery and remodeling 1 year after surgery between LIMA and non-LIMA grafts, the correlation between 1-month shear exposure and 1-year lumen remodeling will be investigated in the next section.

Correlation Between Hemodynamics and Graft Lumen Remodeling

Table 4 shows the relationships between CFD-derived hemodynamic measures taken 1 month post surgery and the percent change in graft lumen diameter 1 year post surgery.

Percent change in graft lumen diameter was not correlated to graft flow rate ($p = 0.106$) nor to average WSS ($p = 0.073$), and plots showing the relationship between these measures can be seen in Fig. 5 and in the Supplemental Materials (Fig. S3). For graft flow rate, arterial grafts generally experienced higher flow rates than SVGs, though flow does not appear to differentiate well between SVGs that experienced a higher degree of lumen remodeling and those that did not. Similarly, many arterial grafts tended to experience higher average WSS compared to SVGs, though some grafts that experienced a low average WSS did not experience much lumen remodeling.

More significantly, unlike other tested hemodynamic measures, abnormal WSS area (< 1 Pa) was found to be correlated to change in graft lumen diameter ($p = 0.030$), with a plot showing their relationship in Fig. 6b and in the Supplemental Materials (Fig. S4b). The grafts that experienced the most inward lumen remodeling during the first year are those that were experiencing higher abnormal WSS area shortly after surgery. On the other hand, grafts that experienced lower abnormal WSS area 1 month post surgery tended to be those that also did not experience much inward remodeling 1 year post surgery. One can also observe a difference in the general behavior of the LIMA grafts, which tended to have both low abnormal WSS area and little 1-year lumen remodeling, compared to the SVGs, which tended to have both high

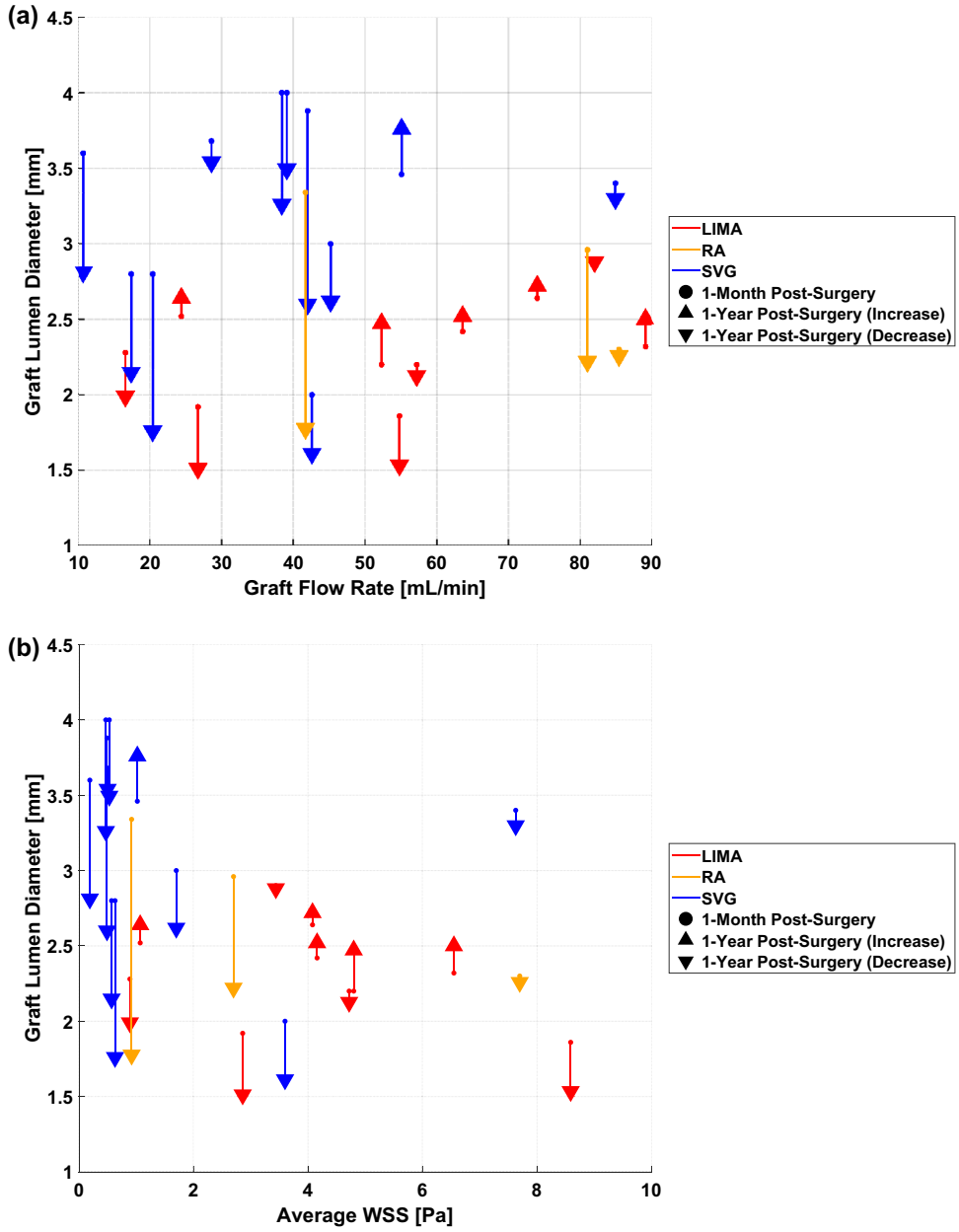

FIGURE 5. Plots relating 1-month graft flow rate (a) and average wall shear stress (b) to 1-month and 1-year graft lumen diameter for LIMA (n = 10), RA (n = 3), and SVG (n = 11). Arrows pointing downwards indicate grafts that have experienced inward lumen remodeling 1 year post surgery, while arrows pointing upwards denote outward remodeling. No significant differences were found in graft flow rate across graft types. Arterial grafts had higher average WSS compared to venous grafts (p = 0.004), with LIMA grafts having higher average WSS than non-LIMA grafts (p = 0.048) and SVG (p = 0.004). Neither graft flow rate nor average WSS were found to correlate to relative change in graft lumen diameter (p = 0.106 and p = 0.073, respectively). *LIMA* left internal mammary artery, *RA* radial artery, *SVG* saphenous vein graft, *WSS* wall shear stress.

abnormal WSS area and more inward lumen remodeling. Additionally, by comparing Figs. 3 and 4, one can see some qualitative association between regions of the SVGs exposed to low WSS area at 1 month post surgery and regions of the same grafts that experienced inward lumen remodeling at 1 year. The qualitative trends for LIMA and RA are unclear.

Interestingly, abnormal WSS area computed with a threshold of < 0.5 Pa was not significantly correlated to change in graft lumen diameter 1 year post surgery ($p = 0.095$). The relationship between these measures

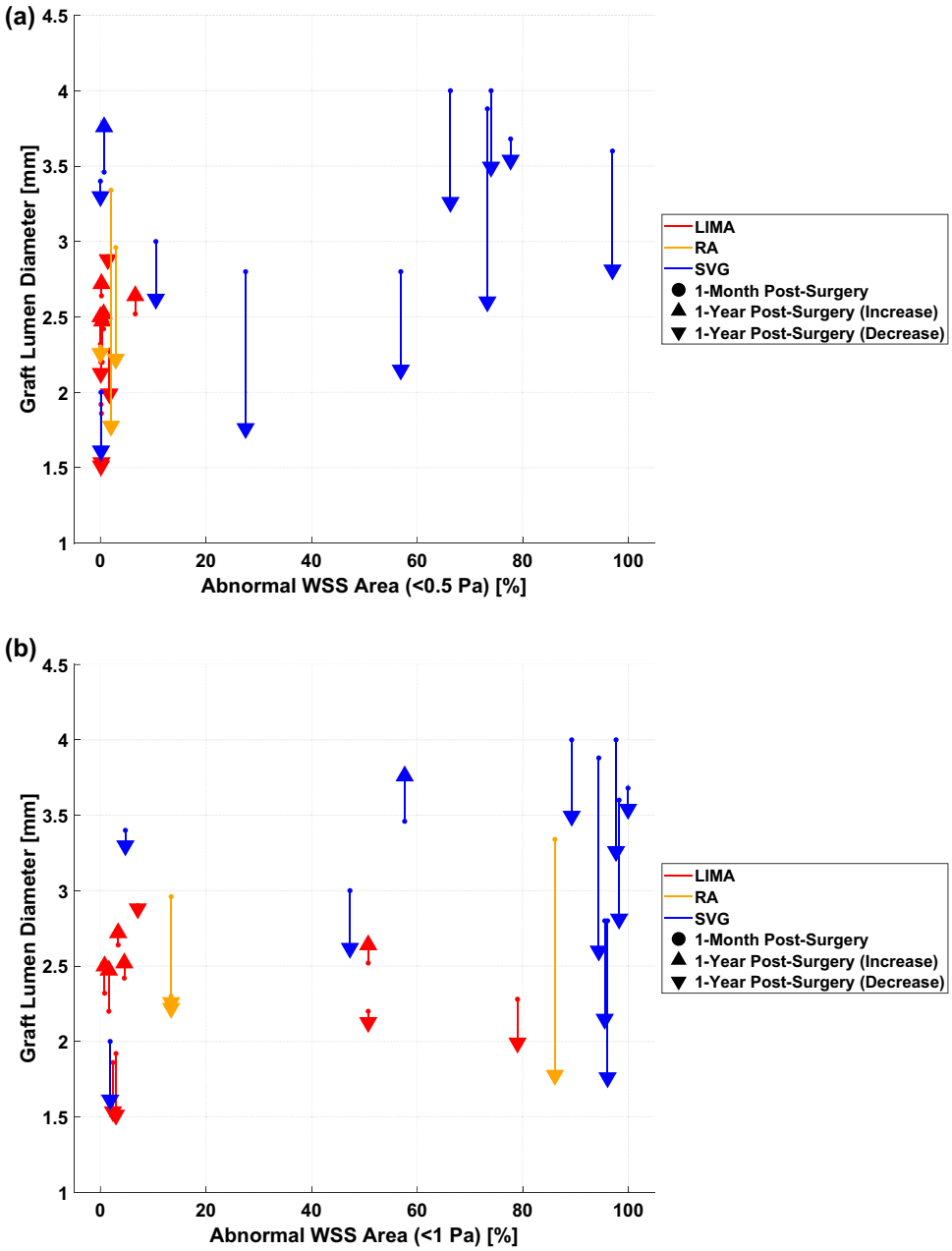

FIGURE 6. Plots relating 1-month abnormal wall shear stress (WSS) area (threshold of < 0.5 Pa in (a), < 1 Pa in (b)) to 1-month and 1-year graft lumen diameter for LIMA (n = 10), RA (n = 3), and SVG (n = 11). Arrows pointing downwards indicate grafts that have experienced inward lumen remodeling 1 year post surgery, while arrows pointing upwards denote outward remodeling. For both the < 0.5 Pa and < 1 Pa thresholds, arterial grafts had lower abnormal WSS area than venous grafts (p = 0.004 for both thresholds), with LIMA grafts having lower abnormal WSS area than both non-LIMA grafts (p = 0.008 and p = 0.004, respectively) and SVG (p = 0.004 and p = 0.001, respectively). Abnormal WSS area with a threshold of < 1 Pa was correlated to relative change in graft lumen diameter (p = 0.030), while the < 0.5 Pa threshold was not (p = 0.095). *LIMA* left internal mammary artery, *RA* radial artery, *SVG* saphenous vein graft.

can be seen in Fig. 6a and in the Supplemental Materials (Fig. S4a). While the grafts exposed to a higher abnormal WSS area (< 0.5 Pa) also tended to experience inward remodeling 1 year post surgery, the 0.5 Pa threshold may be too conservative for differentiating arterial grafts, as all experienced < 10% abnormal WSS area, but some experienced lumen remodeling.

DISCUSSION

In this prospective study, image-guided computational fluid dynamics (CFD) simulations were used to estimate coronary artery bypass graft (CABG) hemodynamics in 10 study participants with 24 bypass grafts one month after surgery. These CFD-derived measures were then compared to the degree of graft lumen

remodeling that occurred one year after surgery. Our results revealed that while graft flow rate was not different among different graft types, arterial grafts experienced higher average wall shear stress (WSS) and lower abnormal WSS area than saphenous vein grafts (SVG). Additionally, left internal mammary artery (LIMA) grafts experienced less inward lumen remodeling one year post surgery compared to non-LIMA grafts and to SVGs. Importantly, we found for the first time prospectively that abnormal WSS area (< 1 Pa) was correlated with the 1-year change in graft lumen diameter, where a higher abnormal WSS area generally corresponds to a higher degree of inward lumen remodeling. This finding suggests that WSS-related mechanisms may play a role in graft remodeling after surgery, which may influence long-term graft failure rates.

Our results are in relatively good agreement with previously reported clinical observations on the relative failure rates among different graft types as well as with previous CFD studies in the context of CABG surgery. SVGs have previously been observed to have higher long-term failure rates than arterial grafts and LIMA grafts.[8,11,21] Hwang *et al.* also showed that WSS measured intraoperatively in CABG patients who received Y-composite grafts consisting of both saphenous vein and LIMA segments negatively correlated to the relative change in diameter one year after surgery, where saphenous vein segments experienced lower intraoperative WSS and greater 1-year diameter reduction compared to the LIMA segments.[14] These clinical observations seem to align with our finding that SVGs have more exposure to abnormally low WSS and experience a greater degree of inward lumen remodeling compared to LIMA grafts.

Additionally, a previous retrospective CFD study performed with images from 5 CABG patients taken 1 to 17 years after surgery demonstrated differences in average WSS and abnormal WSS area between arterial and venous grafts, which align with our findings.[23] A second retrospective CFD study by Khan *et al.* in 15 CABG patients with both healthy and stenosed SVGs showed that WSS normalized by that in a cylindrical vessel with equivalent flow rate and diameter was lower in digitally reconstructed pre-diseased SVG segments than in patent SVGs, also pointing towards shear-related mechanisms for remodeling and potentially failure.[16] Interestingly, their study did not find any significant differences in the abnormal WSS area. This discrepancy could be in part attributed to the authors' graft-specific selection of abnormal WSS threshold, which differs from a common WSS threshold used in the present study. Additionally, the Khan *et al.* study lacked medical images of the pre-stenosed grafts and instead digitally reconstructed their anatomy based on the post-failure images. Our prospective study, on the other hand, based all simulations and analyses on patient medical images taken one month and one year post surgery.

To our knowledge, our work represents one of the larger prospective studies of its kind in applying CFD to CABG surgery, and the use of 4D flow MRI-derived boundary conditions tailors the simulations to be more patient-specific.[7] More significantly, our study is the first to prospectively demonstrate a significant correlation between perioperative graft hemodynamics and post-operative graft remodeling. However, our study has some limitations, including the uncertainties associated with the CT images and 3D model, 4D flow MRI measurements, and vessel wall material properties used for all participants. Furthermore, the anatomical location of the grafts may be a confounding factor, as the *in situ* LIMA grafts in this study were all used to bypass the left anterior descending artery, while SVGs and RA grafts were proximally anastomosed to the ascending aorta and distally anastomosed to other coronary arteries. Additionally, the choice of abnormal WSS threshold (0.5 Pa vs. 1 Pa) influences the correlation between abnormal WSS area and change in lumen diameter found in this study; however, there is currently no single definitive threshold from previous works. Finally, this study related hemodynamic biomarkers to 1-year lumen remodeling rather than graft failure. While graft remodeling can be a precursor to long-term failure, it may also represent a physiological process of the grafts adapting to a different flow environment. Future directions include further longitudinal follow-up of patients in this study to assess clinical outcomes pertaining to graft failure, as well as vascular biology studies to better understand how bypass graft hemodynamics affects cells in the vessel wall.

Overall, our results show for the first time prospectively a correlation between abnormal WSS area (< 1 Pa) 1 month after CABG surgery and the degree of lumen remodeling 1 year post surgery. This correlation suggests that shear-related mechanisms may play a role in short-term graft remodeling. The relation between 1-month hemodynamics and 1-year graft remodeling is important, even though the observed vessel remodeling is not directly associated with graft failure. As different remodeling processes may act at different time points throughout the lifespan of a bypass graft, it is important to study graft remodeling prior to long-term failure to garner a better understanding of how these processes act over time. This study overall contributes to a broader effort to better understand CABG hemodynamics and remodeling, which can lead to improved surgical planning and patient outcomes. In the long term, since our

simulations provide a non-invasive estimate of bypass graft flows and shear stresses, this methodology could eventually be adapted for clinician use to simulate hemodynamic outcomes for hypothetical graft conduit types and placements prior to surgery. Utilizing CFD as an approach to study bypass graft hemodynamics can contribute to a better understanding of the processes leading up to graft failure, which in due course may lead to improvements in clinical practice and surgical outcomes.

SUPPLEMENTARY INFORMATION

The online version contains supplementary material available at https://doi.org/10.1007/s10439-023-03167-4.

ACKNOWLEDGMENTS

This work was supported by the RSNA Scholar Grant #RSCH1716, by the Department of Medical Imaging of the University of Toronto, by the Jean & Lauri Hiivala Research Fund for Heart Health, by the Institute of Biomedical Engineering of the University of Toronto, by the Canada Research Chairs program, and by Compute Canada.

CONFLICT OF INTEREST

No benefits in any form have been or will be received from a commercial party related directly or indirectly to the subject of this manuscript.

REFERENCES

[1]Antiga, L., M. Piccinelli, L. Botti, B. Ene-Iordache, A. Remuzzi, and D. A. Steinman. An image-based modeling framework for patient-specific computational hemodynamics. *Med. Biol. Eng. Comput*. 46:1097, 2008.

[2]Davies, P. F. Hemodynamic shear stress and the endothelium in cardiovascular pathophysiology. *Nat. Clin. Pract. Cardiovasc. Med*. 6:16–26, 2009.

[3]de Graaf, F. R., J. E. van Velzen, A. J. Witkowska, J. D. Schuijf, N. van der Bijl, L. J. Kroft, A. de Roos, J. H. C. Reiber, J. J. Bax, G. J. de Grooth, J. W. Jukema, and E. E. van der Wall. Diagnostic performance of 320-slice multidetector computed tomography coronary angiography in patients after coronary artery bypass grafting. *Eur. Radiol*. 21:2285–2296, 2011.

[4]Eslami, P., J. Tran, Z. Jin, J. Karady, R. Sotoodeh, M. T. Lu, U. Hoffmann, and A. Marsden. Effect of wall elasticity on hemodynamics and wall shear stress in patient-specific simulations in the coronary arteries. *J. Biomech. Eng*. 2019. https://doi.org/10.1115/1.4043722.

[5]Figard, S. Introduction to Biostatistics with JMP. SAS Institute, 2019, 288 pp.at <https://books.google.com/books/about/Introduction_to_Biostatistics_with_JMP.html?id=0ZRMygEACAAJ>.

[6]Figueroa, C. A., I. E. Vignon-Clementel, K. E. Jansen, T. J. R. Hughes, and C. A. Taylor. A coupled momentum method for modeling blood flow in three-dimensional deformable arteries. *Comput. Methods Appl. Mech. Eng*. 195:5685–5706, 2006.

[7]Gallo, D., G. De Santis, F. Negri, D. Tresoldi, R. Ponzini, D. Massai, M. A. Deriu, P. Segers, B. Verhegghe, G. Rizzo, and U. Morbiducci. On the use of *in vivo* measured flow rates as boundary conditions for image-based hemodynamic models of the human aorta: implications for indicators of abnormal flow. *Ann. Biomed. Eng*. 40:729–741, 2012.

[8]Gaudino, M., A. Di Franco, D. L. Bhatt, J. H. Alexander, A. Abbate, L. Azzalini, S. Sandner, G. Sharma, S. V. Rao, F. Crea, S. E. Fremes, and S. Bangalore. The association between coronary graft patency and clinical status in patients with coronary artery disease. *Eur. Heart J*. 42:1433–1441, 2021.

[9]Gijsen, F., Y. Katagiri, P. Barlis, C. Bourantas, C. Collet, U. Coskun, J. Daemen, J. Dijkstra, E. Edelman, P. Evans, K. van der Heiden, R. Hose, B.-K. Koo, R. Krams, A. Marsden, F. Migliavacca, Y. Onuma, A. Ooi, E. Poon, H. Samady, P. Stone, K. Takahashi, D. Tang, V. Thondapu, E. Tenekecioglu, L. Timmins, R. Torii, J. Wentzel, and P. Serruys. Expert recommendations on the assessment of wall shear stress in human coronary arteries: existing methodologies, technical considerations, and clinical applications. *Eur. Heart J*. 40:3421–3433, 2019.

[10]Gimbrone, M. A., and G. García-Cardeña. Endothelial cell dysfunction and the pathobiology of atherosclerosis. *Circ. Res*. 118:620–636, 2016.

[11]Goldman, S., K. Zadina, T. Moritz, T. Ovitt, G. Sethi, J. G. Copeland, L. Thottapurathu, B. Krasnicka, N. Ellis, R. J. Anderson, and W. Henderson. Long-term patency of saphenous vein and left internal mammary artery grafts after coronary artery bypass surgery: Results from a Department of Veterans Affairs Cooperative Study. *J. Am. Coll. Cardiol*. 44:2149–2156, 2004.

[12]Heiberg, E., C. Green, J. Toger, A. M. Andersson, M. Carlsson, and H. Arheden. FourFlow-open source code software for quantification and visualization of time-resolved three-directional phase contrast magnetic resonance velocity mapping. *J. Cardiovasc. Magn. Reson*. 14:W14, 2012.

[13]Heiberg, E., J. Sjögren, M. Ugander, M. Carlsson, H. Engblom, and H. Arheden. Design and validation of segment-freely available software for cardiovascular image analysis. *BMC Med. Imaging*. 10:1, 2010.

[14]Hwang, H. Y., B.-K. Koo, S. Y. Yeom, T. K. Kim, and K.-B. Kim. Endothelial shear stress of the saphenous vein composite graft based on the internal thoracic artery. *Ann. Thorac. Surg*. 105:564–571, 2018.

[15]Jiménez-Juan, L., E. T. Nguyen, B. J. Wintersperger, H. Moshonov, A. M. Crean, D. P. Deva, N. S. Paul, and F. S. Torres. Failed heart rate control with oral metoprolol prior to coronary CT angiography: effect of additional intravenous metoprolol on heart rate, image quality and radiation dose. *Int. J. Cardiovasc. Imaging*. 29:199–206, 2013.

[16]Khan, M. O., J. S. Tran, H. Zhu, J. Boyd, R. R. S. Packard, R. P. Karlsberg, A. M. Kahn, and A. L. Marsden. Low wall shear stress is associated with saphenous vein

graft stenosis in patients with coronary artery bypass grafting. *J. Cardiovasc. Trans. Res.* 2020. https://doi.org/10.1007/s12265-020-09982-7.

[17]Kim, H. J., I. E. Vignon-Clementel, J. S. Coogan, C. A. Figueroa, K. E. Jansen, and C. A. Taylor. Patient-specific modeling of blood flow and pressure in human coronary arteries. *Ann. Biomed. Eng.* 38:3195–3209, 2010.

[18]Lopes, R. D., R. H. Mehta, G. E. Hafley, J. B. Williams, M. J. Mack, E. D. Peterson, K. B. Allen, R. A. Harrington, C. M. Gibson, R. M. Califf, N. T. Kouchoukos, T. B. Ferguson, J. H. Alexander, Project of Ex Vivo Vein Graft Engineering via Transfection IV (PREVENT IV) Investigators. Relationship between vein graft failure and subsequent clinical outcomes after coronary artery bypass surgery. *Circulation.* 125:749–756, 2012.

[19]Markl, M., G. J. Wagner, and A. J. Barker. Re: Blood flow analysis of the aortic arch using computational fluid dynamics. *Eur. J. Cardiothorac. Surg.* 49:1586–1587, 2016.

[20]Petrie, M. C., P. S. Jhund, L. She, C. Adlbrecht, T. Doenst, J. A. Panza, J. A. Hill, K. L. Lee, J. L. Rouleau, D. L. Prior, I. S. Ali, J. Maddury, K. S. Golba, H. D. White, P. Carson, L. Chrzanowski, A. Romanov, A. B. Miller, and E. J. Velazquez. Ten year outcomes after coronary artery bypass grafting according to age in patients with heart failure and left ventricular systolic dysfunction: an analysis of the extended follow up of the STICH trial. *Circulation.* 134:1314–1324, 2016.

[21]Pinho-Gomes, A.-C., L. Azevedo, C. Antoniades, and D. P. Taggart. Comparison of graft patency following coronary artery bypass grafting in the left versus the right coronary artery systems: a systematic review and meta-analysis. *Eur. J. Cardiothorac. Surg.* 54:221–228, 2018.

[22]Pirola, S., Z. Cheng, O. A. Jarral, D. P. O'Regan, J. R. Pepper, T. Athanasiou, and X. Y. Xu. On the choice of outlet boundary conditions for patient-specific analysis of aortic flow using computational fluid dynamics. *J. Biomech.* 60:15–21, 2017.

[23]Ramachandra, A. B., A. M. Kahn, and A. L. Marsden. Patient-specific simulations reveal significant differences in mechanical stimuli in venous and arterial coronary grafts. *J. Cardiovasc. Transl. Res.* 9:279–290, 2016.

[24]Sankaran, S., M. Esmaily Moghadam, A. M. Kahn, E. E. Tseng, J. M. Guccione, and A. L. Marsden. Patient-specific multiscale modeling of blood flow for coronary artery bypass graft surgery. *Ann. Biomed. Eng.* 40:2228–2242, 2012.

[25]Seo, J., A. B. Ramachandra, J. Boyd, A. L. Marsden, and A. M. Kahn. Computational evaluation of venous graft geometries in coronary artery bypass surgery. *Semin. Thorac. Cardiovasc. Surg.* 2021. https://doi.org/10.1053/j.semtcvs.2021.03.007.

[26]Stone, P. H., S. Saito, S. Takahashi, Y. Makita, S. Nakamura, T. Kawasaki, A. Takahashi, T. Katsuki, S. Nakamura, A. Namiki, and A. Hirohata. Prediction of progression of coronary artery disease and clinical outcomes using vascular profiling of endothelial shear stress and arterial plaque characteristics. *Circulation.* 126:172–181, 2012.

[27]Taylor, A. J., et al. ACCF/SCCT/ACR/AHA/ASE/ASNC/NASCI/SCAI/SCMR 2010 appropriate use criteria for cardiac computed tomography. *J. Cardiovasc. Comput. Tomogr.* 4:407.e1-407.e33, 2010.

[28]Taylor, C. A., T. A. Fonte, and J. K. Min. Computational fluid dynamics applied to cardiac computed tomography for noninvasive quantification of fractional flow reserve: scientific basis. *J. Am. Coll. Cardiol.* 61:2233–2241, 2013.

[29]Tran-Nguyen, N., F. Condemi, A. Yan, S. Fremes, P. Triverio, and L. Jimenez-Juan. Wall shear stress differences between arterial and venous coronary artery bypass grafts one month after surgery. *Ann. Biomed. Eng.* 2022. https://doi.org/10.1007/s10439-022-03007-x.

[30]Updegrove, A., N. M. Wilson, J. Merkow, H. Lan, A. L. Marsden, and S. C. Shadden. SimVascular: an open source pipeline for cardiovascular simulation. *Ann. Biomed. Eng.* 45:525–541, 2017.

[31]Zhou, Y., G. S. Kassab, and S. Molloi. On the design of the coronary arterial tree: a generalization of Murray's law. *Phys. Med. Biol.* 44:2929–2945, 1999.

[32]Zientara, A., L. Rings, H. Bruijnen, O. Dzemali, D. Odavic, A. Häussler, M. Gruszczynski, and M. Genoni. Early silent graft failure in off-pump coronary artery bypass grafting: a computed tomography analysis†. *Eur. J. Cardiothorac. Surg.* 56:919–925, 2019.